Carbohydrate Polymers 107 (2014) 110–118

Contents lists available at ScienceDirect

Carbohydrate Polymers

journal homepage: www.elsevier.com/locate/carbpol

Various-sourced pectin and polyethylene oxide electrospun fibers

Pamela L. Rockwell, Marjorie A. Kiechel, Jennifer S. Atchison, Laura J. Toth, Caroline L. Schauer*

Department of Materials Science and Engineering, Drexel University, Philadelphia, PA 19104, USA

ARTICLE INFO

Article history:
Received 20 December 2013
Received in revised form 23 January 2014
Accepted 5 February 2014
Available online 22 February 2014

Keywords:
Pectin
Electrospinning
Citrus peel
Apple pomace
Sugar beet pulp
Polygalacturonic acid

ABSTRACT

Pectin, a naturally occurring and biorenewable polysaccharide, is derived from plant cell wall tissue and used in applications ranging from food processing to biomedical engineering. Due to extraction methods and source variation, there is currently no consensus in literature as to the exact structure of pectin. Here, we have studied key material properties of electrospun pectin blends with polyethylene oxide (PEO) (1:1, v/v) in order to demonstrate the fabrication of a fibrous and less toxic material system, as well as to understand the effects of source variability on the resulting fibrous mats. The bulk pectin degree of esterification (DE) estimated using FTIR (bulk apple pomace (AP) = 28%, bulk citrus peel (CP) = 86% and bulk sugar beet pulp (SBP) = 91%) was shown to inversely correlate with electrospun fiber crystallinity determined using XRD (PEO–AP = 37%, PEO–CP = 28% and PEO–SBP = 23%). This in turn affected the trend observed for the mean fiber diameter ($n = 50$) (PEO–AP = 124 ± 26 nm, PEO–CP = 493 ± 254 nm and PEO–SBP = 581 ± 178 nm) and elastic tensile moduli (1.6 ± 0.2 MPa, 4.37 ± 0.64 MPa and 2.49 ± 1.46 MPa, respectively) of the fibrous mats. Electrospun fibers containing bulk AP had the lowest DE, highest crystallinity, smallest mean fiber diameter, and lowest tensile modulus compared to either the bulk CP or bulk SBP. Bound water in PEO–CP fiber and bulk pectin impurities in PEO–SPB were observed to influence fiber branching and mean diameter distributions, which in turn influenced the fiber tensile properties. These results indicate that pectin, when blended with PEO in water, produces submicron fibrous mats with pectin influencing the blend fiber properties. Moreover, the source of pectin is an important variable in creating electrospun blend fibrous mats with desired material properties.

1. Introduction

Pectin, one of the most complex heterogeneous polysaccharides in nature, is composed of mainly (98%) linear chains of (1,4)-linked-α-D-galacturonic acid (or homogalacturonan (HGA)) (Yapo, 2011a). Additionally, it also contains other pectic domains namely, rhamnogalacturonan-I (RG-I) (Yapo, 2011b), rhamnogalacturonan-II or xylogalacturonan (XGA) (Pelloux, Rusterucci, & Mellerowicz, 2007; Yapo, 2011a). Four pectin structure models have been reported in the literature (*i.e.* precursor rhamnogalacturonan; traditional alternating regions of HGA and RG-I model; RG-I backbone' and the 'living thing like' models (Yapo, 2011a)) with the most cited pectin model as composed of a primarily HGA backbone alternating with RG-I backbone. Its common features can be grouped into two major domains: "smooth" regions consisting of the HGA and "hairy" regions consisting of RG-I and/or XGA linkages (Yapo, 2011a). Instead of the HGA, the third model proposed an RG-I backbone structure while a more recent hypothetical model included both HGA and RG-I in its core (Yapo, 2011a).

While the exact arrangement of these components is source-dependent, the widely accepted pectin functionality is the partial esterification of the abundant D-galacturonic acid residues with either methyl groups at the C6 position and/or acetyl groups at O2 and/or O3 positions (Pelloux et al., 2007; Yapo, 2011a). Although the RG-I domains ([2)-α-L-rhamnose-(1,4)-α-D-galacturonic acid-(1] contain D-galacturonic acid residues, there is limited evidence that it is methyl-esterified (Fellah, Anjukandi, Waterland, & Williams, 2009).

The degree of esterification (DE) or the number of methoxy groups (low (LM) or high (HM)) substituting the carboxylic acid (COOH) moiety on the galacturonic acid residues is often used to classify the different types of pectin (*i.e.* low DE (or LM) < *ca.* 42.9% < high DE (or HM)) as it influences the gelation mechanism, processing conditions and properties of the polymer (Thakur, Singh, & Handa, 1997; Voragen, Coenen, Verhoef, & Schols, 2009). It has been observed in plants that a low percentage of methyl DE (*i.e.* high COO^-) form ionic bridges with positively charged Ca^{2+}, influencing

* Corresponding author at: 3141 Chestnut Street, LeBow 439A, Philadelphia, PA 19104, USA. Tel.: +1 215 895 6797; fax: +1 215 895 6760.
E-mail addresses: cschauer@coe.drexel.edu, cschauer@drexel.edu (C.L. Schauer).

http://dx.doi.org/10.1016/j.carbpol.2014.02.026
0144-8617/

cell wall mechanical properties and porosity (Ridley, O'Neill, & Mohnen, 2001; Wolf, Mouille, & Pelloux, 2009). High DE pectins on the other hand are known to form stable gels by a combination of intermolecular hydrogen bonds and hydrophobic interactions (Thakur et al., 1997).

Commercially available pectin is extracted from various dicotyledonous plant sources including apple pomace (AP) (Canteri-Schemin, Fertonani, Waszczynskyj, & Wosiacki, 2005), citrus peel (CP) (Alexander & Sulebele, 1980) and sugar beet pulp (SBP) (Dea & Madden, 1986). Traditional models of the structure of AP, CP and SBP suggest that in a given chain, AP has the longest smooth region interrupted by a few hairy regions with XGA at the end and/or middle of the chain (Coenen, Bakx, Verhoef, Schols, & Voragen, 2007), CP has a medium length smooth region with few hairy regions consisting of mostly RG-I at the end-chain (Zhan, Janssen, & Mort, 1998) while SBP has many short length smooth regions with the most hairy regions of mostly RG-I on both ends of the chain (Oosterveld, Voragen, & Schols, 2002).

Pectin is extensively utilized as a gelling agent in the food technology and processing industries. However, the inconsistencies in chemical structure due to commercial extraction methods and inherent source variability have limited its use in other applications. Non-food applications of pectin include its incorporation in the design of hydrogels (Guan, Shao, & Yao, 1996), films/coatings (Shu, Zhu, & Song, 2001) for controlled drug release or as ion-specific electrodes (Cataldo, Gianguzza, Pettignano, Piazzese, & Sammartano, 2012). Because of its abundance, cost, biodegradability, water-solubility, non-toxicity, bioadhesive property, ion-specific complexation capability and reactive and/or charged functional groups, pectin still represents an attractive natural material for various biomedical, pharmaceutical, electrochemical and reactive chemical device applications.

Electrospinning is a simple and flexible fiber-forming technique that utilizes electrical instead of mechanical forces to draw fibers out of a polymer solution or melt (Reneker & Chun, 1996; Reneker, Yarin, Fong, & Koombhongse, 2000). A basic electrospinning setup requires only three essential parts: advancement pump, conductive target and a high voltage source. The positive end of the voltage source is usually wired to the polymer solution/melt that is placed at a set distance away from the target, which in turn is connected to the other end of the voltage source. The growing interest in polymer electrospinning stems from the capacity of the technique to produce continuous, controllable and uniform fibers with diameters reaching the nanometer scale (Reneker & Yarin, 2008). The high surface area-to-volume ratio renders the 3D fibrous mat more attractive with broader material properties such as increased porosity and available surface for chemical modifications and interactions. Improvements in these fiber properties have driven research geared toward a wide range of applications which include membrane filtration (Barhate & Ramakrishna, 2007; Ma, Kotaki, & Ramakrishna, 2005), biosensing (Sawicka, Gouma, & Simon, 2005), tissue scaffold engineering (Matthews, Wnek, Simpson, & Bowlin, 2002; Wnek, Carr, Simpson, & Bowlin, 2003) and drug delivery (Goldberg, Langer, & Jia, 2007).

Electrospun natural polysaccharide fibers of chitin (Min et al., 2004), chitosan (Austero, Donius, Wegst, & Schauer, 2012; Ohkawa, Cha, Kim, Nishida, & Yamamoto, 2004; Schiffman & Schauer, 2007), cellulose acetate (Liu & Hsieh, 2002) or gelatin/hyaluronic acid (Li et al., 2006) have been widely reported. However, two common challenges encountered when processing natural polymers by electrospinning are: (1) solvent choice and (2) need for additional carrier polymers. Due to their solvent insolubility and strong polymer interchain hydrogen bonding, natural polymers are often electrospun in more toxic, if not more corrosive solvents, than those used for synthetic polymer fiber spinning. As a consequence, additional laborious and costly post-processing steps to remove the solvent or neutralize the mat are necessary to render the fibers suitable for applications that require biocompatibility. Additionally, fabricating fibers from only natural polymers has been a challenge due to their complex chain chemistries and solution properties. The latter is often easily addressed by blending the fibers with commonly electrospun synthetic carrier polymers. Polyethylene oxide (PEO), a linear semicrystalline polymer, is often the polymer blend of choice due to its biocompatibility, fiber spinning reproducibility and water solubility, which is favorable when there is a need to selectively remove PEO from the mat. Previously, PEO and pectin fibers were produced by electrospinning the blend polymer from solutions containing aqueous NaOH/folic acid/sodium alginate (Alborzi, Lim, & Kakuda, 2010; Alborzi, Lim, & Kakuda, 2013) or chloroform (Furlan et al., 2012). Instead, this study utilized water as a non-toxic, biocompatible and inexpensive solvent alternative for electrospinning PEO–pectin polymer blends.

Here, we aim to develop a fibrous, and less toxic, material system that exploits both the rich functionality of the various sources of pectin and the unique structural morphology produced during electrospinning. Specifically, we investigate the production of these fine fibers from various pectin sources – AP, CP and SBP blended with a biocompatible and water-soluble carrier – PEO to determine how the addition of various pectin types to the electrospun blend solution influences the chemical interactions, crystallinity, surface morphology and tensile properties of the fibers.

2. Materials and methods

2.1. Reagents

Citrus peel (CP, M_W = 170–230 kDa, DE = 36.4%) and sugar beet pulp pectin (SBP, Genu® Beta Pectin, M_W = ~200 kDa, DE = ~55%) samples were generously donated by C.P. Kelco (Atlanta, GA, USA). Sodium chloride (NaCl), sodium hydroxide (NaOH), hydrochloric acid (HCl), methanol (MeOH), apple pectin (AP, P2157, M_W = 30–100 kDa, methoxy group ≥ 7.1%) and polyethylene oxide (PEO, M_W = 600 kDa) were purchased from Sigma Aldrich, MO, USA. DE values here were obtained from the certificate of analysis or data from the bulk powder suppliers. All bulk samples were used as received. All aqueous solutions were prepared with doubly distilled water.

2.2. Preparation of bulk citrus pectin with varying DE

The DE of bulk CP was modified using similar methods as those utilized by Limberg et al. for the base catalyzed deesterification of pectin. Briefly, bulk CP (12.5 g) was mixed into a hot NaCl (0.546 g)/water solution (400 mL). The mixture was stirred for 1 h and cooled in an ice bath (2–3 °C) and kept below 4 °C. The acidity of the solution was adjusted to pH 9 using a 1 M NaOH and maintained at this pH until desired DE was achieved.

To prepare bulk CP with DE greater than about 40% (CP-HDE), the reaction was stopped by lowering the solution acidity to pH 2.8 using 4 M HCl. CP-HDE was precipitated using isopropanol (500 mL) and then air dried (23–25 °C and 21–32% relative humidity).

To prepare bulk CP with DE lower than about 40% (CP–LDE), the mixture was allowed to form voluminous precipitates using 2 M HCl and then kept below 5 °C for 24 h. The precipitate was filtered with cloth and washed in suspension for 2 h using a MeOH (80 mL)/2 M HCl (100 mL) solution. The precipitate was filtered again and washed in suspension for 2 h with 200 mL 1:1 MeOH/water. The precipitate (CP–LDE) was then washed with a final solution of 200 mL 67:33 MeOH/water. Residual washings were filtered and removed by pressing the precipitate firmly.

CP-LDE was oven dried (23–25 °C) for 20 h and then air dried right after (23–25 °C and 21–32% relative humidity).

2.3. Preparation of electrospinning solutions

Aqueous 3 wt% solutions of PEO, AP, CP and SBP were mixed separately. All solutions were mixed for 24 h at room temperature on an Arma Rotator A-1 (Bethesda, MD, USA). Blends containing 1:1 volume ratios of PEO–AP, PEO–CP, PEO–SBP were prepared prior to electrospinning.

2.4. Preparation of electrospun PEO–pectin fiber

All blend solutions were individually loaded into a 10 mL disposable syringe (Becton Dickinson & Co., Franklin Lakes, NJ, USA) with a 21-gauge needle (Becton Dickinson & Co., Franklin Lakes, NJ, USA) attached. Electrospinning was performed under a set flow rate of 20 μL/min (Harvard Apparatus, Plymouth Meeting, PA, USA), with a fixed 10 cm needle tip to collector distance and with 18 kV applied (Gamma High Voltage Research Inc., Ormond Beach, FL, USA) to the needle. The fibers were collected under ambient conditions of 23–25 °C and 21–32% relative humidity. As controls, pure PEO mats were also electrospun under the same conditions. Prior to characterization, the fiber mats were carefully peeled off an aluminum foil collector wrapped around a copper mesh electrode and stored under ambient conditions.

2.5. Bulk powder and solution characterization

Infrared spectra of all dry bulk pectin powders were taken using FTIR (Varian Excalibur FTS-3000, Varian, Inc., Palo Alto, CA) under attenuated total reflectance (ATR) mode. Scans were taken over a spectral range of 4000–500 cm^{-1} with 4 cm^{-1} wavenumber resolution and an average of 64 scans. To estimate the DE of the bulk AP, CP and SBP, two common spectral methods were utilized: (1) DE_1 (%) = [peak area of esterified carboxylic groups at 1720 cm^{-1}/total number of carboxylic groups peak area at 1720 cm^{-1} and 1600 cm^{-1}] × 100, where 1720 cm^{-1} peak is assumed to be solely due to esterified carboxylic acid (Chatjigakis et al., 1998); and (2) DE_2 (%) = [peak area of ester CH_3 asymmetric stretch at 1400 cm^{-1}] peak of 1010 cm^{-1} backbone vibration (Fellah et al., 2009).

The pH of the aqueous blend solutions were determined using a universal range (pH 0–14) indicator sticks (J.T. Baker, Deventer, Netherlands). Measurements were performed in triplicates and under ambient temperature (23 ± 3 °C).

Crystallinity of the dry bulk powders were determined using an X-ray diffractometer (Rigaku SmartLab) with $Cu_{K\alpha}$ = 1.54 Å radiation operating at 40 kV and 30 mA. Scans were taken at 5–50° at a step rate of 0.04°/s and 2 s duration for each step. The percent crystallinity (%) was recorded after taking the ratio of the area under the curve of the crystalline peak and the total area of the peaks (amorphous + crystalline) and reporting the values in percentages.

2.6. Characterization of fiber chemical interactions

Crystallinity and FTIR spectra of the dry electrospun PEO–pectin fibers were measured similar to the method described for the bulk powder samples.

2.7. Fiber surface morphology characterization

The morphology of the spun fibers were imaged with a Zeiss Supra 50VP field emission scanning electron microscope (FESEM, Carl Zeiss NTS, LLC, North America) after coating with platinum/palladium for 35 s and 40 mA using Denton Vacuum Desk II (Denton Vacuum, LLC, Moorestown, NJ, USA). Mean fiber diameters (n = 50) were determined using the ImageJ software (version 1.41o, National Institute of Health, USA). Statistical analyses were all performed using a StatPlus:Mac LE.2009 (Build 5.8.0.0, AnalystSoft Inc.) with p-level < 0.05 for significance.

2.8. Fiber tensile property characterization

Initial tensile properties of the spun mats were measured using an Instron 5500R (Model 1125, Instron, Norwood, MA, USA). Mat strips measuring 10 mm × 35 mm were mounted with a double-sided tape in square paper frames having a 25 mm × 25 mm opening. Before applying tension, the frames were clamped with pneumatic grips and cut on both vertical sides to allow for the loading of the sample at the start of the test. Tests were performed using a 5 N load cell at a strain rate of 0.02 s^{-1}. Load values were converted to stress by estimating the effective thickness from the mass per unit area of the mat, assuming a density of the fiber material of 1210 kg/m^3 and 895 kg/m^3 for PEO and PEO–pectin blends, respectively. Young's modulus was determined from the initial linear elastic slope of the stress–strain curve.

3. Results and discussion

3.1. Bulk powder and solution characterization

Fig. 1 displays a schematic of the smooth and hairy regions found in pectins that are typically derived from AP, CP and SBP sources, while Fig. 2 exhibits the chemical structures of polygalacturonan (methyl or acetyl esterified or unesterified), rhamnose and xylose units found in the smooth region and hairy regions (RG-I, RG-II or XGA) of various pectins, respectively. In this study and for ease and convenience in comparing with majority of data available in literature, we assume that the pectin structure follows the traditional model (*i.e.* smooth region as main chain and interrupted by hairy regions). FTIR spectra (Fig. 3) of the dry bulk pectin powder displayed the characteristic pectin peaks at around 1720 cm^{-1} (C═O of ester and carboxylic acid), 1600 cm^{-1} (COO^- stretch) and 1395 cm^{-1} (C—O—H bend). The bands at 1313 cm^{-1} and 1219 cm^{-1} are attributed to C—H deformation while bands at 1130 cm^{-1}, 1076 cm^{-1} and 1007 cm^{-1} are contributed by the C—O—C symmetric stretch, C—C bonds of the polymer backbone chain and the C—O stretch of the esters (Chatjigakis et al., 1998; Fellah et al., 2009; Gnanasambandam & Proctor, 2000; Kaczmarek, Bajer, Galka, & Kotnowska, 2007; Monsoor, 2005; Venyaminov & Kalnin, 1990). A closer look at the bulk AP spectrum also reveal three differences compared to bulk CP and bulk SBP spectra: C—O—H bend is at a higher wavenumber (1420 cm^{-1}) due to H-bonding; additional peaks at 1352 cm^{-1} and 1259 cm^{-1} owing to ether linkages; and 1130 cm^{-1} which is more like a shoulder than a distinct peak and some additional peaks at 1053 cm^{-1} and 1030 cm^{-1} due to other types of sugar rings in pectin.

Bulk AP, CP and SBP displayed varied intensities of the ester carbonyl–carboxylate ion (Chatjigakis et al., 1998) peaks or the peaks for the CH_3 deformation–backbone vibration (Fellah et al., 2009), indicative of differences in DE. Previous reports on the determination of an accurate DE value from FTIR data have been challenging due to the possible interference from either bound water or carboxylates and other ester groups from phenolics, which are also abundant in and extracted from plant cell walls (Fellah et al., 2009). Although the O—CH_3 of the methoxyl ester group gives a strong FTIR peak (Supplementary Figure 1) at around 2950–2750 cm^{-1}, this is not usually used to quantify DE as it is often masked by the strong and broad O—H stretch of the

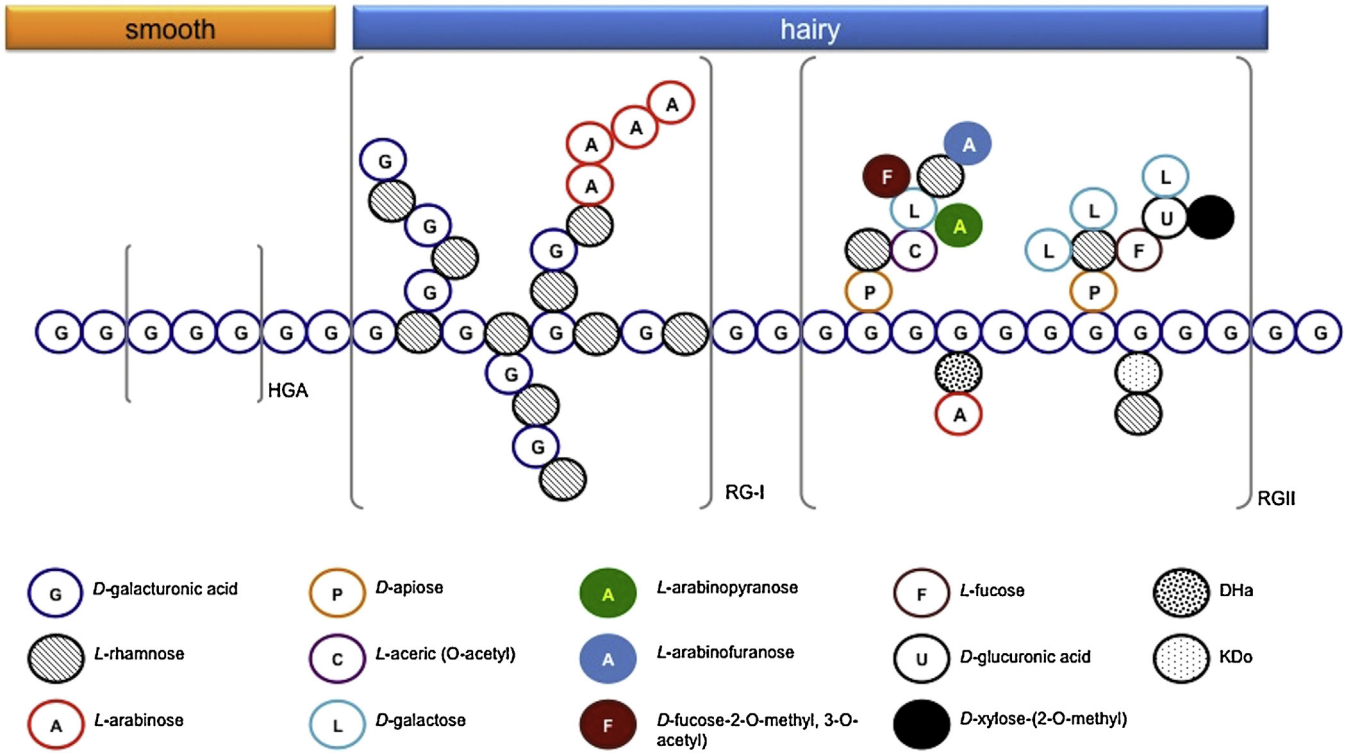

Fig. 1. Traditional model of the structure of pectin displaying the homogalacturonan (HGA) as the backbone and smooth region and interrupted by the hairy region consisting of rhamnogalacturonan-I (RG-I) or rhamnogalacturonan-II (RG-II) units. The lengths of the smooth and hairy regions are dependent on the pectin source and method of extraction. Two newer models of pectin structure proposed were: (1) smooth region is a branch of the hairy regions consisting of the main chain, or (2) hairy and smooth regions are separate chains but exists as copolymers.

intramolecular hydrogen bonds of the polymer and bound water (Gnanasambandam & Proctor, 2000).

Supplementary material related to this article can be found, in the online version, at http://dx.doi.org/10.1016/j.carbpol.2014.02.026.

We attempted to estimate the DE using two spectral methods to better understand our starting material and determine which method correlates well with the trends observed on the fiber properties. Table 1 summarizes the estimated DE based on the two previously described methods, the pectin type and the bulk aqueous solution pH of the samples.

The first method (DE_1) relies on the 1720 cm^{-1} (ester) and 1600 cm^{-1} (COO^-) bands (Chatjigakis et al., 1998; Gnanasambandam & Proctor, 2000). The increased ester carbonyl peak intensity and width coupled by decreased carboxylate ion band intensity often denotes partial esterification of the *D*-galacturonan residues. The estimated DE_1 of bulk AP is the highest (DE_1 = 56%), bulk CP as the least (DE_1 = 14%) and bulk SBP

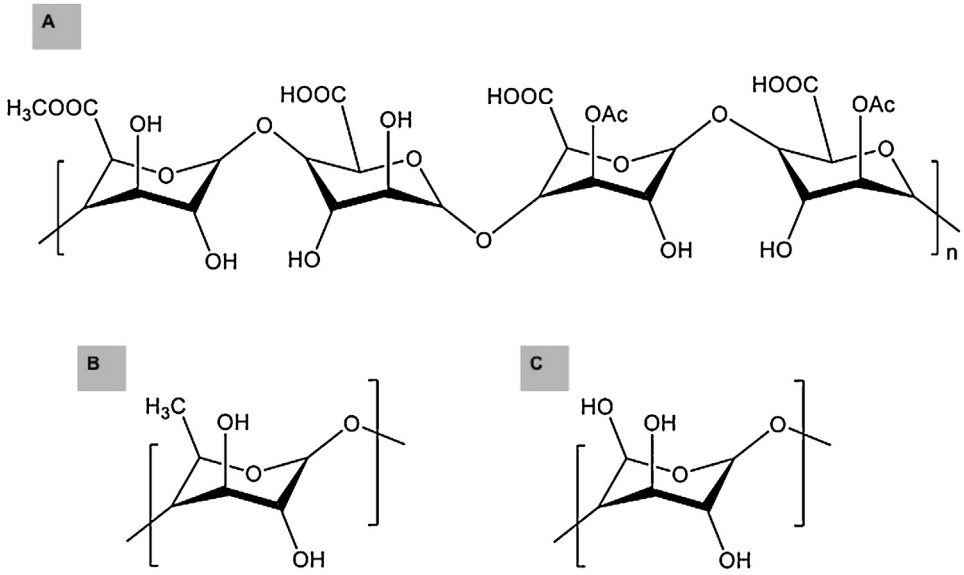

Fig. 2. Chemical structures of (A) polygalacturonic acid showing the subunits containing either the methyl ester at C6 or the acetyl ester at O2 and/or O3, (B) rhamnose subunit that is present on the RG-I and RG-I domains, and (C) xylose subunit.

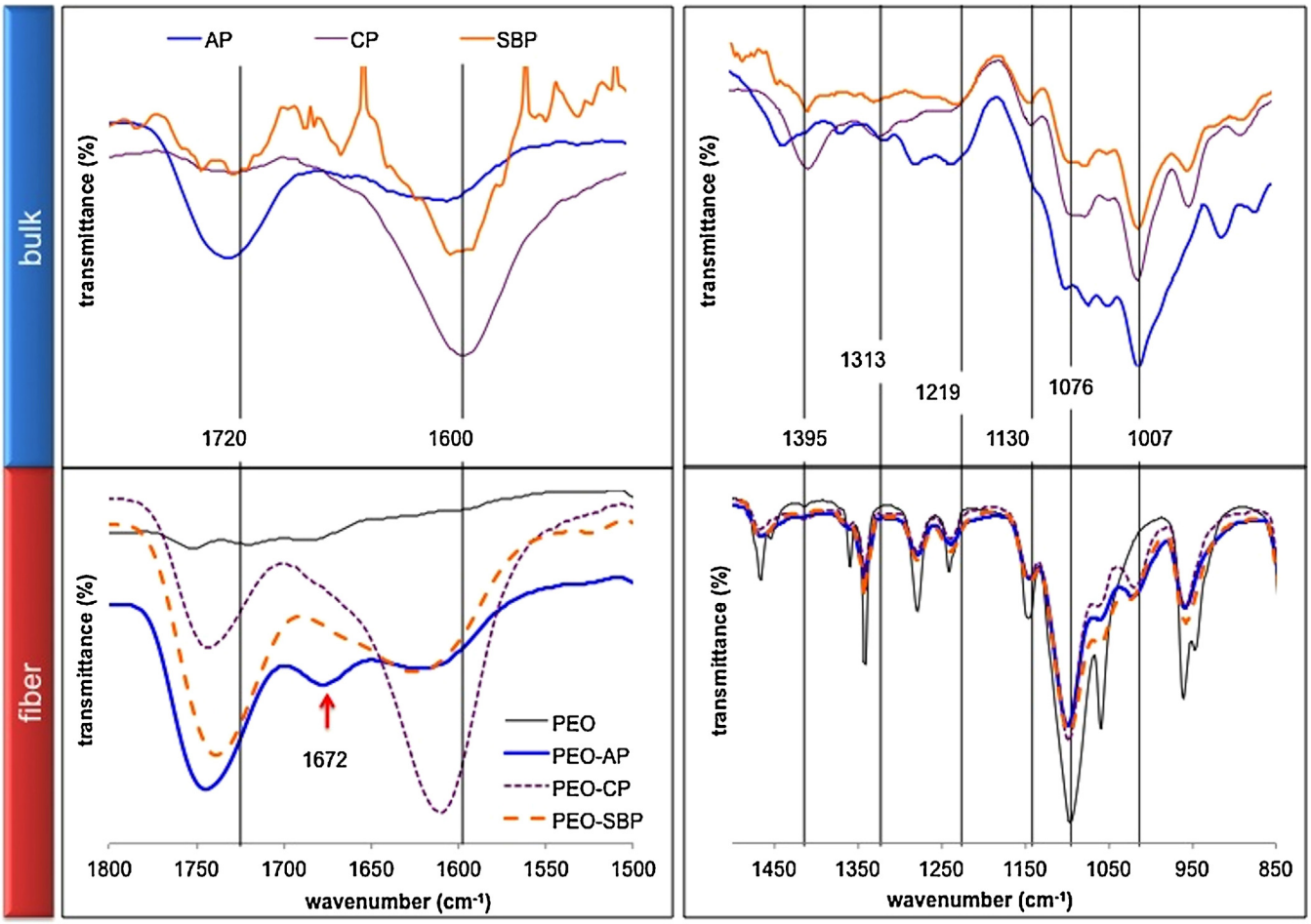

Fig. 3. FTIR spectra of bulk pectin powder from apple pomace (AP), citrus peel (CP) and sugar beet pulp (SBP) and its electrospun fibers with PEO. Characteristic peaks of pectin are denoted by the black solid vertical line at 1720 cm^{-1} and black dashed vertical line at 1600 cm^{-1} for the carbonyl (C=O) of the ester and carboxylic acid and the carboxylic anion (COO^-) asymmetrical stretches, respectively. Additional peaks at 1395 cm^{-1} denote C—O—H bend and bands at 1313 cm^{-1} and 1219 cm^{-1} are attributed to C—H deformation while bands at 1130 cm^{-1}, 1076 cm^{-1} and 1007 cm^{-1} are contributed by the C—O—C symmetric stretch and C—C bonds of the backbone chain.

as intermediate (DE_1 = 31%). Using the HM or LM criteria, the bulk AP is considered HM while the bulk CP and bulk SBP are LM. This method however may be disadvantageous since absorption of these functional groups is dependent on the presence of ions, water and changes in acidity (Fellah et al., 2009). Moreover, this method does not take into account the presence of other carbonyl groups that are not part of the smooth main chain but may contribute to the infrared absorbance.

The pH values of the 3 wt% aqueous pectin solutions correlated to the DE_1 estimates. Pectins generally have a $pK_{a(COOH)}$ of 3.3–4.5 (Michel, Thibault, & Doublier, 1984; Ravanat & Rinaudo, 1980), so at this pH, the ionizable carboxylic acid (*i.e.* unesterified) groups are ~50% protonated. Since the ester group does not ionize in solution, then any changes in pH can be attributed to the protonation or deprotonation of the COOH (unesterified) groups. The pH of AP, CP and SBP aqueous solutions were 3.0, 4.5 and 3.5, respectively, indicating that both AP and SBP exist in mostly COOH form while CP is in mostly COO^- form, which correlates with the FTIR bulk powder spectra and hence, the DE_1 values. Changes in pH and presence of water however would influence these estimates. At our solution electrospinning conditions (~pH 3–4), the COOH in pectin is partially protonated and the typical carboxylic acid group IR absorption (1750 cm^{-1}) then absorbs at the same energy as the esterified moieties (1740 cm^{-1}) – leading to poor estimates of the DE_1 if the 1740 cm^{-1} is assumed to be solely due to the ester carbonyl. Obtaining the most accurate estimate using the DE_1 method would then require manipulation of the COOH groups to be fully charged or deprotonated (high pH) – which when performed to our bulk powder would be a challenge when comparing to bands of the PEO–pectin blend fibers (low pH).

Fellah et al. (2009) suggested an alternative but more robust approach that eliminated the issues encountered when estimating DE from hydrated or low pH samples. Instead of the carbonyl groups, the bands corresponding to the asymmetric CH_3 stretch mode (1395 cm^{-1}) and the backbone vibration (1007 cm^{-1}) were utilized (Fellah et al., 2009; Synytsya, Copikova, Matejka, & Machovic, 2003). Values obtained, based on the DE_2 method, have previously shown good correlation with classical DE estimates, even though the backbone vibration band used is attributed solely to the HGA and considering pectin contains other sugars

Table 1
Estimated DE_1 (%) and DE_2 (%) values of bulk AP, CP and SBP and their corresponding methoxy type and pH in aqueous solutions.

Pectin type	FTIR estimated DE and type[a]		DE (%) from supplier	pH[b]
	DE_1 (%)	DE_2 (%)		
AP	55.85 (HM)	28.34 (LM)	>7.10	3.0
CP	14.13 (LM)	85.54 (HM)	36.4	4.5
SBP	30.76 (LM)	90.66 (HM)	~55.0	3.5

[a] Low methoxy (LM) < 42.9% < high methoxy (HM).
[b] Measurements were taken as 3 wt% pectin in water.

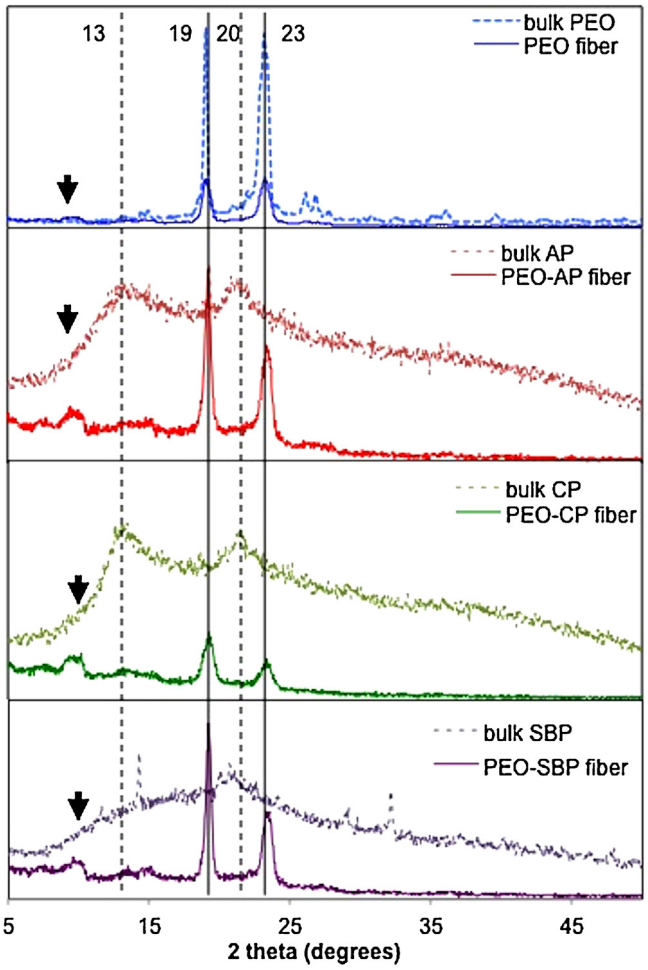

Fig. 4. XRD spectra of bulks and electrospun PEO–pectin blend fibers. Pectin characteristic peaks are at $2\theta = 13^\circ$ and 20° (vertical black dashed lines). PEO characteristic peaks are at $2\theta = 19^\circ$ and 23° for the 120 and 112 plane, respectively (black vertical solid lines). The peak at $2\theta = \sim 9^\circ$ (black arrow) denotes oriented intermolecular bonds in electrospun fibers.

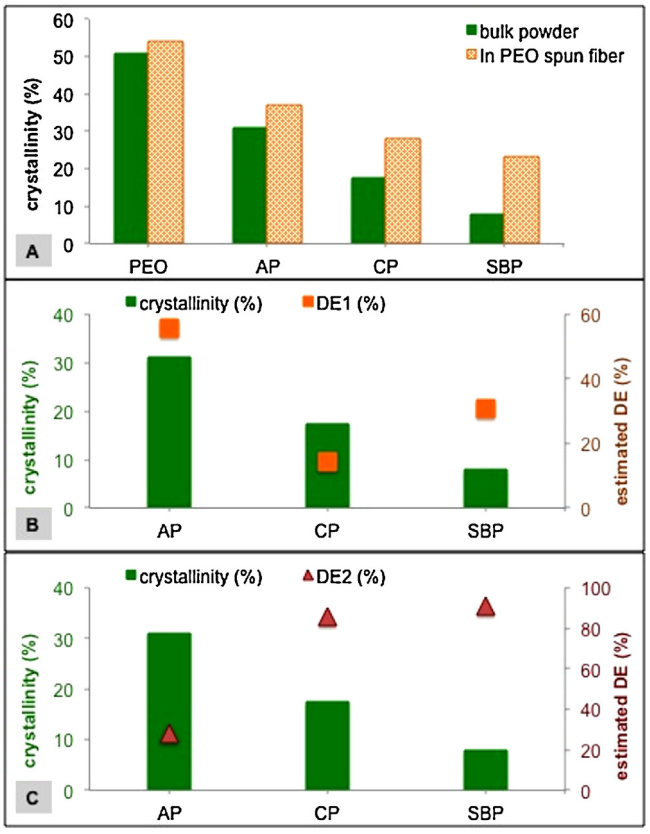

Fig. 5. Plots of the (A) percent crystallinity (%) of bulk PEO and pectin from apple pomace (AP), citrus peel (AP) and sugar beet pectin (SBP) and their corresponding electrospun blend fiber. (B) Percent crystallinity of bulk pectins and its corresponding estimated DE1 (%) and (C) DE2 (%) values.

in its chain (those in RG-I, RG-II or XGA components). In this study, the values estimated by the DE_2 method were different from DE_1 values, namely the bulk AP was the least esterified ($DE_2 = 28\%$), bulk CP was intermediate ($DE_2 = 86\%$) and bulk SBP the most ($DE_2 = 91\%$) esterified. This trend agrees with the suggested arrangement and number of smooth and hairy regions found in AP (#long smooth > #hairy), CP (#intermediate length smooth > #hairy) and SBP (#short smooth ≈ hairy) pectin sources (Coenen et al., 2007; Oosterveld et al., 2002; Voragen et al., 2009; Yapo, 2011a; Zhan, Janssen, & Mort, 1998) (Fig. 1). These values also correspond to bulk AP having a low methoxyl (LM) content while bulk CP and SBP have high methoxyl contents (Table 1). Although the DE_2 values do not agree with the supplier DE values, we suggest the DE_2 method is a better estimate of number of methoxyl groups for our bulk pectin compared to DE_1 values, therefore a more accurate DE because the CH_3 and backbone vibrations are not influenced by hydration and acidity. These major differences in DE and the structure of the various components from various sources greatly influence pectin material properties.

Fig. 4 displays the XRD spectra of the bulk PEO and pectin powders and the corresponding PEO–pectin blend fiber while Fig. 5 summarizes their respective % crystallinity and estimated DE calculated from the two spectral methods. The PEO characteristic peaks were observed at $2\theta = 19^\circ$ and 23° corresponding to the 120 and 112 plane, respectively. PEO is semicrystalline, denoted by the narrower peaks than those of pectin. Here, bulk PEO powder is 51% crystalline – typical of the polymer.

Pectin characteristic reflections are at $2\theta = 13^\circ$ and $\sim 20^\circ$ (Sharma & Ahuja, 2011; Sutar, Mishra, Pal, & Banthia, 2008). Depending on the number of pectin domains and bound water in the sample, the reflections may shift to higher or lower angles (Tsami, Vagenas, & Marinoskouris, 1992; Zykwinska, Rondeau-Mouro, Garnier, Thibault, & Ralet, 2006). A shift to higher angles indicates reduced lattice parameter that may be due to the presence of lower defects (*i.e.* can be low number of hairy regions or impurities) or higher backbone smooth region chain alignment. Pectins are generally semicrystalline (Panchev, Slavov, Nikolova, & Kovacheva, 2010; Zykwinska et al., 2006) but with much lower crystalline phase than PEO. Bulk AP, bulk CP and bulk SBP % crystallinity was determined to be 31%, 17% and 8%, respectively. The number of domains (HGA, RG-I, RG-II or XGA) has been previously shown to contribute to the shifts and reflection patterns in pectin. The $2\theta = 13^\circ$ peak, suggesting an interatomic distance of about 3.42 Å for the HGA domains (smooth region), was observed as a broad peak for bulk AP and bulk CP but was not observed for bulk SBP. In contrast to bulk AP and bulk CP, this low crystallinity in addition to the shift to lower angles of the $2\theta = 20^\circ$ peak may be due to the presence of impurities and/or the short length and high distribution of hairy regions on the chain that influences order on the smooth region in bulk SBP. These bulk SBP impurities were also observed in its bulk FTIR spectrum (Fig. 3) may act as defects, reducing its crystalline phase.

Lower crystallinity was also observed for bulk pectins having high DE_2, while the DE_1 estimates did not show any correlation with the % crystallinity (Fig. 5). In the presence of methoxyl groups

during esterification (*i.e.* high DE), the chain–chain alignment between the smooth regions (crystalline phase) are disrupted which may result to an increase in its amorphous phase with the methoxyl groups acting as intermolecular spacers (Tsami et al., 1992). The crystallinity data observed for our bulk supports our suggestion that DE_2 is a closer estimate than DE_1.

The bulk samples were then electrospun into random meshes with the PEO carrier in aqueous solutions to determine how these various chemistries play a role in fiber surface morphologies and mat mechanical properties.

3.2. Fiber chemical interactions

All aqueous solutions containing PEO–AP, PEO–CP and PEO–SBP blends produced random fibrous network mats. FTIR (Fig. 3) spectra of the electrospun fibers suggest that pectin, spun with the PEO carrier, contributed to the chemical interactions of the entire blend fiber. Spectrum of the PEO fiber display its characteristic peaks (Guo, Liu, Wang, & Chen, 1999; Kaczmarek, Bajer, Galka, & Kotnowska, 2007; Marcos, Orlandi, & Zerbi, 1990; Rocco, Pereira, & Felisberti, 2001; Su, Wang, & Liu, 2002): 2640–3080 cm^{-1} owing to CH_2 stretching (Supplementary Figure 1); 1464 cm^{-1} (CH scissoring), 1359 cm^{-1} + 1340 cm^{-1} (CH wagging), 1240 cm^{-1} (CH twisting), 958 cm^{-1} (CH rocking) which are indicative of ordered PEO (helical and triclinic unit cells). Moreover, the ether (C—O—C) stretching was likewise observed as three medium–strong bands at 1144 cm^{-1}, 1092 cm^{-1} and 1059 cm^{-1}, all suggesting the ordered structure of PEO in the fiber.

In the blend fibers, although PEO bands were more intense than those of pectin, the characteristic bands from both polymers were observed suggesting fiber formation of pectin with PEO from aqueous solutions. These pectin bands from the electrospun fiber are evident on the 1800–1500 cm^{-1} region where none of the PEO functional groups are active. Here, pectin bands shifted due to intra-, interchain and van der Waals interactions with other pectin molecules or with PEO (Safi, Morshed, Ravandi, & Ghiaci, 2007; Su et al., 2002). This shift allowed a better understanding of the pectin functionalities. The 1740 cm^{-1}, 1610 cm^{-1} (previously 1720 cm^{-1} and 1600 cm^{-1}) and the 1672 cm^{-1} bands give an idea of how the carbonyl groups of pectin interact with the solvent and the PEO chain. In solution, these peaks also give more information regarding the DE of our pectin types. PEO–AP fibers displayed a more pronounced 1672 cm^{-1} peak that is assigned the carboxylic acid (COOH) group, which leaves 1740 cm^{-1} and 1610 cm^{-1} for the $COOCH_3$ and the COO^- peaks, respectively. The presence of the 1672 cm^{-1} (COOH) band in PEO–AP further confirms that the bulk AP pectin used has the lowest DE of the three types. For both PEO–CP and PEO–SBP, the 1672 cm^{-1} band was not observed and this can be attributed to the high DE (*i.e.* less COOH) and/or the presence of the ionic form of pectin in the fibers. Structural changes in PEO–SBP fibers also suggested chain or solvent interactions as observed on the peak shifts. Unlike PEO–AP, PEO–SBP (suggested to have the highest DE2) did not display COOH peak in the blend fiber.

XRD spectra of the electrospun fibers are displayed in Fig. 4 while Fig. 5 displays the calculated % crystallinity of the electrospun blend fibers. Due to the intensity of the PEO reflections, the influence of the various pectins on the crystallinity of the blend fibers was only observed in the changes in PEO characteristic peak intensities at $2\theta = 19^\circ$ and 23° for the 120 and 112 planes. The percent crystallinity of the PEO fibers with various pectin follow the same trend bulks and is inversely related to the DE: PEO–AP (37%) > PEO–CP (28%) > PEO–SBP (23%). After electrospinning, the PEO mats maintained their semicrystalline microstructure and even displayed a small increase in % crystallinity (51% in bulk to 54% in fiber) due to alignment during fiber formation, although the process has been reported to decrease crystallinity by reducing orientation along the 112 plane (Shi, Zhou, Liao, & Wang, 2005). Similarly, 112 plane peak decay was observed but with blend samples and was achieved by the addition of the various types of pectin. Pectin may have disrupted PEO crystal formation due to intermolecular chain entanglements or chain interactions. In this study, the addition of a pectin type with a higher DE leads to PEO–pectin fibers with lower crystallinity. This was expected since even in bulk samples, the higher DE samples have more structural defects that lower the ability of the chain to have uniform orientation within a plane. In contrast to bulk samples however, electrospun fibers (with and without the addition of pectin) produced fibers that have higher percent crystallinity. Additionally, formation of a new peak at $2\theta = \sim 9$ was observed only on spun fibers and is suggested to be due to the oriented intermolecular H-bonding during electrospinning.

3.3. Fiber surface morphology

All solutions prepared were able to produce fibers by electrospinning. Fig. 6 displays the representative FESEM micrographs and mean diameters of the fibers spun from all the blends and the PEO solution, respectively. The addition of the various types of pectin yielded fibers that were round and smooth. All fiber diameters were in the submicron range with either PEO–SBP (581 ± 178 nm) or PEO–CP (493 ± 254 nm) fibers being significantly larger ($p < 0.05$) than PEO (285 ± 57 nm). In contrast, the PEO–AP fibers (124 ± 26 nm) were significantly smaller ($p < 0.05$) than PEO.

Interestingly, the mean fiber diameters of the electrospun PEO–pectin blends were influenced by the crystallinity (DE_2) and the charge on the carboxylic acid (COOH or COO^-). Addition of pectins with lower DE_2 produced fibers with smaller mean fiber diameters. Moreover, PEO–AP and PEO–SBP fibers were unbranched while PEO–CP is more web-like (Fig. 6). The branching is likely a result of the ionic form of the pectin. Branching and web-like morphologies of electrospun fibers are known to influence the mechanical and chemical properties of the material (Donius, Kiechel, Schauer, & Wegst, 2013).

Crystallinity and the presence of ionic form and impurities from the bulk powder influenced the fiber diameter distribution as well. Fibers spun from more crystalline polymer and blend solutions (PEO and PEO–AP) displayed small fiber diameters with a narrow fiber diameter distribution, while those spun from less crystalline blends (PEO–CP and PEO–SBP) produced larger fibers and a wider distribution of sizes. Wong et al. have observed that increased crystallinity of electrospun poly-ε-caprolactone fibers correlated with smaller fiber diameters. Based upon XRD results, the bulk AP powder and PEO–AP fibers were more crystalline compared to the other pectin sources, which may have contributed to smaller fiber diameters (Lutz, Aserin, Wicker, & Garti, 2009; Wong, Baji, & Leng, 2008). These are all indicative of the presence of pectin in the fibers and its strong influence in the overall fiber structure and morphology.

3.4. Fiber tensile property

Young's moduli and tensile strengths of the electrospun fibers are displayed in Fig. 7. Similar to the fiber diameter distribution, the trend observed during the unidirectional tensile test could also be arranged based on the pectin type that was used – either semicrystalline with a low DE (bulk AP) or less crystalline with higher DE (bulk CP or bulk SBP). Fibers produced from PEO–CP and PEO–SBP exhibited higher tensile moduli (92–117 MPa) and tensile strengths (2–4 MPa) than PEO–AP ($E = 21 \pm 5$ MPa and $\sigma_{UTS} = 1.60 \pm 0.20$ MPa) fibers, a semicrystalline pectin. This is in agreement with literature in that more crystalline phases may reduce the tensile properties of fibers. Also, the PEO–CP, being more web-like has more fiber–fiber contact points that contributes to increased tensile modulus and

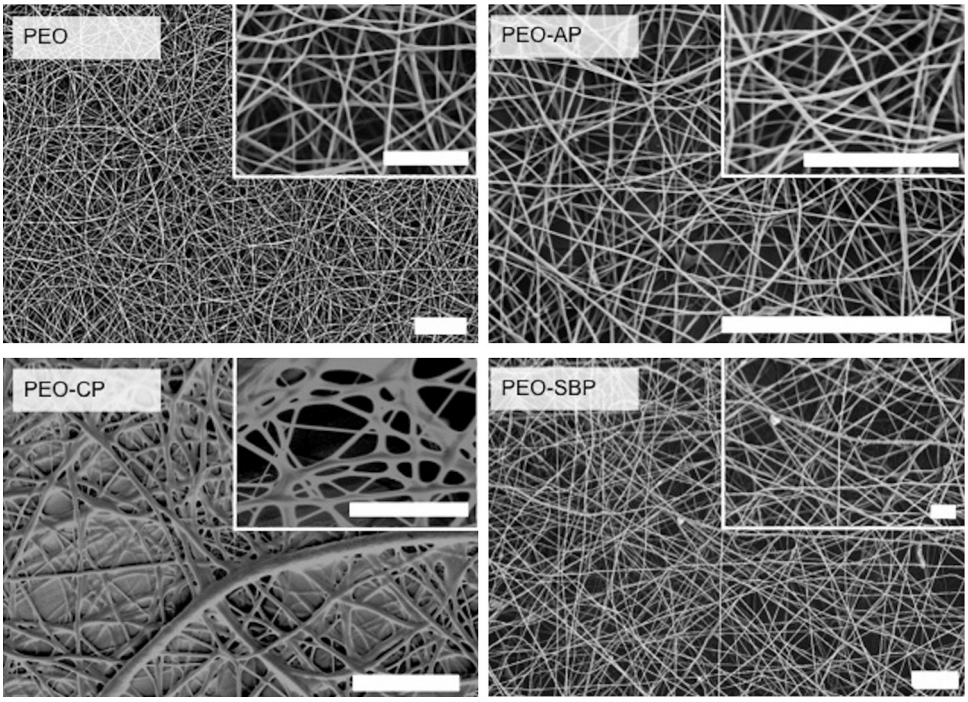

Fig. 6. Representative FESEM micrographs of electrospun PEO (285 ± 57 nm), PEO–AP (124 ± 26 nm), PEO–CP (493 ± 254 nm) and PEO–SBP (581 ± 178 nm) blend fibers. Scale bars on main images are 10 μm and 5 μm for insets.

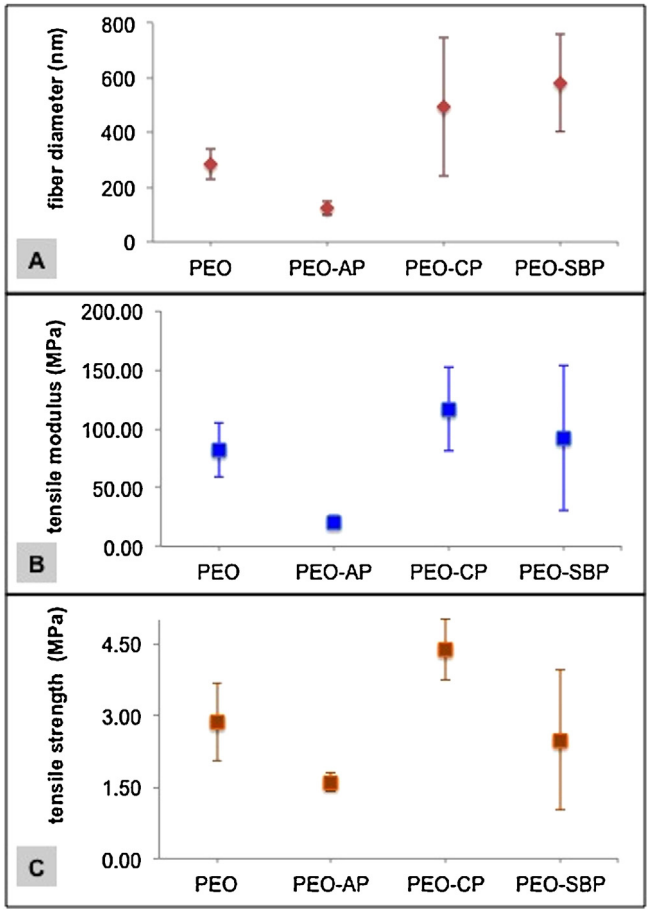

Fig. 7. Plots of the (A) mean fiber diameter, (B) tensile modulus and (C) tensile strength of electrospun PEO, PEO–AP, PEO–CP and PEO–SBP fibers.

strengths, similar to fibers our previously spun charged polymer fibers (Donius et al., 2013; Kiechel & Schauer, 2013).

4. Conclusion

Production of fine fibers of PEO and various-sourced pectin from aqueous blend solutions by electrospinning was demonstrated. The submicron-diameter range distributions, tensile moduli and strengths of the collected fibers were influenced by both the degree of esterification (DE_2) and the crystallinity of the bulk pectins. Addition of the higher DE and less crystalline bulk SBP and bulk CP types produced PEO blend fibers with larger fiber diameters with wider distribution and higher tensile moduli and strength. In contrast, addition of the semicrystalline bulk AP type produced fibers that possessed smaller diameters and a narrower size distribution with a lower tensile modulus and strength compared to that of bulk SBP and bulk CP. These various pectin-based fibrous membranes can have applications in devices that require materials with increased surface area and sensitivity to slight pH or metal ion concentrations such as in electrochemical devices, drug delivery or controlled release and postoperative adhesion membrane applications.

Acknowledgements

The authors thank: Drexel University Centralized Research Facilities (CRF), for use of the FESEM, sputter coater and XRD; Shan Cheng and Dr. Christopher Y. Li for assistance and use of the XRD; Dr. Giuseppe Palmese for the use of the ATR-FTIR; Dr. Christopher Pastore and the Philadelphia University for use of the Instron 5500R; PLR thanks Jacqueline Compton of CP Kelco and LinShu Liu, Marshall Fishman and Arland Hotchkiss of the USDA ERRC. MAK thanks the Institute of Food Technologists (Philadelphia section), Drexel University Freshmen Design Engineering Fellowship 2010–2013 and Drexel University Office of Graduate Studies Dissertation Fellowship; LJT thanks GAANN PHARMA AY 2012–2013, College of Engineering Office of Graduate Students Fellowship. JSA would like

to thank Drexel University Freshmen Design Engineering Fellowship 2011–2012.

References

Alborzi, S., Lim, L. T., & Kakuda, Y. (2010). Electrospinning of sodium alginate–pectin ultrafine fibers. *Journal of Food Science*, *75*(1), C100–C107.

Alborzi, S., Lim, L. T., & Kakuda, Y. (2013). Encapsulation of folic acid and its stability in sodium alginate–pectin–poly(ethylene oxide) electrospun fibres. *Journal of Microencapsulation*, *30*(1), 64–71.

Alexander, M. M., & Sulebele, G. A. (1980). Characterization of pectins from Indian citrus peels. *Journal of Food Science and Technology-Mysore*, *17*(4), 180–182.

Austero, M. S., Donius, A. E., Wegst, U. G. K., & Schauer, C. L. (2012). New crosslinkers for electrospun chitosan fibre mats. I. Chemical analysis. *Journal of the Royal Society Interface*, *9*(75), 2551–2562.

Barhate, R. S., & Ramakrishna, S. (2007). Nanofibrous filtering media: Filtration problems and solutions from tiny materials. *Journal of Membrane Science*, *296*(1–2), 1–8.

Canteri-Schemin, M. H., Fertonani, H. C. R., Waszczynskyj, N., & Wosiacki, G. (2005). Extraction of pectin from apple pomace. *Brazilian Archives of Biology and Technology*, *48*(2), 259–266.

Cataldo, S., Gianguzza, A., Pettignano, A., Piazzese, D., & Sammartano, S. (2012). Complex formation of copper(II) and cadmium(II) with pectin and polygalacturonic acid in aqueous solution. An ISE-H+ and ISE-Me2+ electrochemical study. *International Journal of Electrochemical Science*, *7*(8), 6722–6737.

Chatjigakis, A. K., Pappas, C., Proxenia, N., Kalantzi, O., Rodis, P., & Polissiou, M. (1998). FT-IR spectroscopic determination of the degree of esterification of cell wall pectins from stored peaches and correlation to textural changes. *Carbohydrate Polymers*, *37*(4), 395–408.

Coenen, G. J., Bakx, E. J., Verhoef, R. P., Schols, H. A., & Voragen, A. G. J. (2007). Identification of the connecting linkage between homo- or xylogalacturonan and rhamnogalacturonan type I. *Carbohydrate Polymers*, *70*(2), 224–235.

Dea, I. C. M., & Madden, J. K. (1986). Acetylated pectic polysaccharides of sugar beet. *Food Hydrocolloids*, *1*(1), 71–88.

Donius, A. E., Kiechel, M. A., Schauer, C. L., & Wegst, U. G. K. (2013). New crosslinkers for electrospun chitosan fibre mats. Part II: Mechanical properties. *Journal of the Royal Society Interface*, *10*(81)

Fellah, A., Anjukandi, P., Waterland, M. R., & Williams, M. A. K. (2009). Determining the degree of methylesterification of pectin by ATR/FT-IR: Methodology optimisation and comparison with theoretical calculations. *Carbohydrate Polymers*, *78*(4), 847–853.

Furlan, R., Rosado, J. A. M., Rodriguez, G. G., Fachini, E. R., da Silva, A. N. R., & da Silva, M. L. P. (2012). Formation and characterization of oriented micro-and nanofibers containing poly (ethylene oxide) and pectin. *Journal of the Electrochemical Society*, *159*(3), K66–K71.

Gnanasambandam, R., & Proctor, A. (2000). Determination of pectin degree of esterification by diffuse reflectance Fourier transform infrared spectroscopy. *Food Chemistry*, *68*(3), 327–332.

Goldberg, M., Langer, R., & Jia, X. Q. (2007). Nanostructured materials for applications in drug delivery and tissue engineering. *Journal of Biomaterials Science – Polymer Edition*, *18*(3), 241–268.

Guan, Y. L., Shao, L., & Yao, K. D. (1996). A study on correlation between water state and swelling kinetics of chitosan-based hydrogels. *Journal of Applied Polymer Science*, *61*(13), 2325–2335.

Guo, C., Liu, H. Z., Wang, J., & Chen, J. Y. (1999). Conformational structure of triblock copolymers by FT-Raman and FTIR spectroscopy. *Journal of Colloid and Interface Science*, *209*(2), 368–373.

Kaczmarek, H., Bajer, K., Galka, P., & Kotnowska, B. (2007). Photodegradation studies of novel biodegradable blends based on poly(ethylene oxide) and pectin. *Polymer Degradation and Stability*, *92*(11), 2058–2069.

Kiechel, M. A., & Schauer, C. L. (2013). Non-covalent crosslinkers for electrospun chitosan fibers. *Carbohydrate Polymers*, *95*, 123–133.

Li, J. X., He, A. H., Han, C. C., Fang, D. F., Hsiao, B. S., & Chu, B. (2006). Electrospinning of hyaluronic acid (HA) and HA/gelatin blends. *Macromolecular Rapid Communications*, *27*(2), 114–120.

Liu, H. Q., & Hsieh, Y. L. (2002). Ultrafine fibrous cellulose membranes from electrospinning of cellulose acetate. *Journal of Polymer Science Part B – Polymer Physics*, *40*(18), 2119–2129.

Lutz, R., Aserin, A., Wicker, L., & Garti, N. (2009). Structure and physical properties of pectins with block-wise distribution of carboxylic acid groups. *Food Hydrocolloids*, *23*(3), 786–794.

Ma, Z. W., Kotaki, M., & Ramakrishna, S. (2005). Electrospun cellulose nanofiber as affinity membrane. *Journal of Membrane Science*, *265*(1–2), 115–123.

Marcos, J. I., Orlandi, E., & Zerbi, G. (1990). Poly(ethylene oxide) poly(methyl methacrylate) interactions in polymer blends – An infrared study. *Polymer*, *31*(10), 1899–1903.

Matthews, J. A., Wnek, G. E., Simpson, D. G., & Bowlin, G. L. (2002). Electrospinning of collagen nanofibers. *Biomacromolecules*, *3*(2), 232–238.

Michel, F., Thibault, J. F., & Doublier, J. L. (1984). Viscometric and potentiometric study of high-methoxyl pectins in the presence of sucrose. *Carbohydrate Polymers*, *4*(4), 283–297.

Min, B. M., Lee, S. W., Lim, J. N., You, Y., Lee, T. S., Kang, P. H., et al. (2004). Chitin and chitosan nanofibers: Electrospinning of chitin and deacetylation of chitin nanofibers. *Polymer*, *45*(21), 7137–7142.

Monsoor, M. A. (2005). Effect of drying methods on the functional properties of soy hull pectin. *Carbohydrate Polymers*, *61*(3), 362–367.

Ohkawa, K., Cha, D. I., Kim, H., Nishida, A., & Yamamoto, H. (2004). Electrospinning of chitosan. *Macromolecular Rapid Communications*, *25*(18), 1600–1605.

Oosterveld, A., Voragen, A. G. J., & Schols, H. A. (2002). Characterization of hop pectins shows the presence of an arabinogalactan-protein. *Carbohydrate Polymers*, *49*(4), 407–413.

Panchev, I. N., Slavov, A., Nikolova, K., & Kovacheva, D. (2010). On the water-sorption properties of pectin. *Food Hydrocolloids*, *24*(8), 763–769.

Pelloux, J., Rusterucci, C., & Mellerowicz, E. J. (2007). New insights into pectin methylesterase structure and function. *Trends in Plant Science*, *12*(6), 267–277.

Ravanat, G., & Rinaudo, M. (1980). Investigation on oligogalacturonic and polygalacturonic acids by potentiomatry and circular-dichroism. *Biopolymers*, *19*(12), 2209–2222.

Reneker, D. H., & Chun, I. (1996). Nanometre diameter fibres of polymer, produced by electrospinning. *Nanotechnology*, *7*(3), 216–223.

Reneker, D. H., & Yarin, A. L. (2008). Electrospinning jets and polymer nanofibers. *Polymer*, *49*(10), 2387–2425.

Reneker, D. H., Yarin, A. L., Fong, H., & Koombhongse, S. (2000). Bending instability of electrically charged liquid jets of polymer solutions in electrospinning. *Journal of Applied Physics*, *87*(9), 4531–4547.

Ridley, B. L., O'Neill, M. A., & Mohnen, D. A. (2001). Pectins: Structure, biosynthesis, and oligogalacturonide-related signaling. *Phytochemistry*, *57*(6), 929–967.

Rocco, A. M., Pereira, R. P., & Felisberti, M. I. (2001). Miscibility, crystallinity and morphological behavior of binary blends of poly(ethylene oxide) and poly(methyl vinyl ether-maleic acid). *Polymer*, *42*(12), 5199–5205.

Safi, S., Morshed, M., Ravandi, S. A. H., & Ghiaci, M. (2007). Study of electrospinning of sodium alginate, blended solutions of sodium alginate/poly(vinyl alcohol) and sodium alginate/poly(ethylene oxide). *Journal of Applied Polymer Science*, *104*(5), 3245–3255.

Sawicka, K., Gouma, P., & Simon, S. (2005). Electrospun biocomposite nanofibers for urea biosensing. *Sensors and Actuators B – Chemical*, *108*(1–2), 585–588.

Schiffman, J. D., & Schauer, C. L. (2007). One-step electrospinning of cross-linked chitosan fibers. *Biomacromolecules*, *8*(9), 2665–2667.

Sharma, R., & Ahuja, M. (2011). Thiolated pectin: Synthesis, characterization and evaluation as a mucoadhesive polymer. *Carbohydrate Polymers*, *85*(3), 658–663.

Shi, T. J., Zhou, Y. B., Liao, R. G., & Wang, H. L. (2005). Studies on dispersing morphology and crystallization behavior of electrospun poly (ethylene oxide) fibers. *Acta Polymerica Sinica*, *5*, 760–763.

Shu, X. Z., Zhu, K. J., & Song, W. H. (2001). Novel pH-sensitive citrate cross-linked chitosan film for drug controlled release. *International Journal of Pharmaceutics*, *212*(1), 19–28.

Su, Y. L., Wang, J., & Liu, H. Z. (2002). Melt, hydration, and micellization of the PEO–PPO–PEO block copolymer studied by FTIR spectroscopy. *Journal of Colloid and Interface Science*, *251*(2), 417–423.

Sutar, P. B., Mishra, R. K., Pal, K., & Banthia, A. K. (2008). Development of pH sensitive polyacrylamide grafted pectin hydrogel for controlled drug delivery system. *Journal of Materials Science-Materials in Medicine*, *19*(6), 2247–2253.

Synytsya, A., Copikova, J., Matejka, P., & Machovic, V. (2003). Fourier transform Raman and infrared spectroscopy of pectins. *Carbohydrate Polymers*, *54*(1), 97–106.

Thakur, B. R., Singh, R. K., & Handa, A. K. (1997). Chemistry and uses of pectin – A review. *Critical Reviews in Food Science and Nutrition*, *37*(1), 47–73.

Tsami, E., Vagenas, G. K., & Marinoskouris, D. (1992). Moisture sorption isotherms of pectins. *Journal of Food Processing and Preservation*, *16*(3), 151–161.

Venyaminov, S. Y., & Kalnin, N. N. (1990). Quantitative IR spectrophotometry of peptide compounds in water (H_2O) solutions. 1. Spectral parameters of amino-acid residue absorption-bands. *Biopolymers*, *30*(13-14), 1243–1257.

Voragen, A. G. J., Coenen, G.-J., Verhoef, R. P., & Schols, H. A. (2009). Pectin, a versatile polysaccharide present in plant cell walls. *Structural Chemistry*, *20*(2), 263–275.

Wnek, G. E., Carr, M. E., Simpson, D. G., & Bowlin, G. L. (2003). Electrospinning of nanofiber fibrinogen structures. *Nano Letters*, *3*(2), 213–216.

Wolf, S., Mouille, G., & Pelloux, J. (2009). Homogalacturonan methyl-esterification and plant development. *Molecular Plant*, *2*(5), 851–860.

Wong, S. C., Baji, A., & Leng, S. W. (2008). Effect of fiber diameter on tensile properties of electrospun poly(epsilon-caprolactone). *Polymer*, *49*(21), 4713–4722.

Yapo, B. M. (2011a). Pectic substances: From simple pectic polysaccharides to complex pectins – A new hypothetical model. *Carbohydrate Polymers*, *86*(2), 373–385.

Yapo, B. M. (2011b). Rhamnogalacturonan-I: A structurally puzzling and functionally versatile polysaccharide from plant cell walls and mucilages. *Polymer Reviews*, *51*(4), 391–413.

Zhan, D. F., Janssen, P., & Mort, A. J. (1998). Scarcity or complete lack of single rhamnose residues interspersed within the homogalacturonan regions of citrus pectin. *Carbohydrate Research*, *308*(3-4), 373–380.

Zykwinska, A., Rondeau-Mouro, C., Garnier, C., Thibault, J. F., & Ralet, M. C. (2006). Alkaline extractability of pectic arabinan and galactan and their mobility in sugar beet and potato cell walls. *Carbohydrate Polymers*, *65*(4), 510–520.